AMERICAN SOCIETY FOR MICROBIOLOGY | Infection and Immunity®

BACTERIAL INFECTIONS

Purine Biosynthesis Metabolically Constrains Intracellular Survival of Uropathogenic *Escherichia coli*

Carrie L. Shaffer,[a]* Ellisa W. Zhang,[a]* Anne G. Dudley,[b] Beverly R. E. A. Dixon,[c,d] Kirsten R. Guckes,[a] Erin J. Breland,[a] Kyle A. Floyd,[a] Daniel P. Casella,[b] Holly M. Scott Algood,[a,c,d] Douglass B. Clayton,[b] Maria Hadjifrangiskou[a,b]

Department of Pathology, Microbiology and Immunology, Vanderbilt University School of Medicine, Nashville, Tennessee, USA[a]; Division of Pediatric Urology, Vanderbilt University Medical Center, and Monroe Carell Jr. Children's Hospital at Vanderbilt, Nashville, Tennessee, USA[b]; Department of Medicine, Vanderbilt University School of Medicine, Nashville, Tennessee, USA[c]; Veterans Affairs Tennessee Valley Healthcare System, Nashville, Tennessee, USA[d]

ABSTRACT The ability to *de novo* synthesize purines has been associated with the intracellular survival of multiple bacterial pathogens. Uropathogenic *Escherichia coli* (UPEC), the predominant cause of urinary tract infections, undergoes a transient intracellular lifestyle during which bacteria clonally expand into multicellular bacterial communities within the cytoplasm of bladder epithelial cells. Here, we characterized the contribution of the conserved *de novo* purine biosynthesis-associated locus *cvpA-purF* to UPEC pathogenesis. Deletion of *cvpA-purF*, or of *purF* alone, abolished *de novo* purine biosynthesis but did not impact bacterial adherence properties *in vitro* or in the bladder lumen. However, upon internalization by bladder epithelial cells, UPEC deficient in *de novo* purine biosynthesis was unable to expand into intracytoplasmic bacterial communities over time, unless it was extrachromosomally complemented. These findings indicate that UPEC is deprived of purine nucleotides within the intracellular niche and relies on *de novo* purine synthesis to meet this metabolic requirement.

KEYWORDS *E. coli*, UPEC, bladder, intracellular, urinary tract infection

Received 3 June 2016 **Returned for modification** 9 July 2016 **Accepted** 10 October 2016

Accepted manuscript posted online 17 October 2016

Citation Shaffer CL, Zhang EW, Dudley AG, Dixon BREA, Guckes KR, Breland EJ, Floyd KA, Casella DP, Algood HMS, Clayton DB, Hadjifrangiskou M. 2017. Purine biosynthesis metabolically constrains intracellular survival of uropathogenic *Escherichia coli*. Infect Immun 85:e00471-16. https://doi.org/10.1128/IAI.00471-16.

Editor Shelley M. Payne, University of Texas at Austin

Address correspondence to Maria Hadjifrangiskou, maria.hadjifrangiskou@vanderbilt.edu.

* Present address: Carrie L. Shaffer, Department of Biology and Biological Engineering, California Institute of Technology, Pasadena, California, USA; Ellisa W. Zhang, St. Louis College of Pharmacy, St. Louis, Missouri, USA.

Numerous bacterial pathogens gain entry into nonphagocytic host cells, where they reside unperturbed by host defenses and antibiotic intervention. Upon uptake, intracellular pathogens such as *Salmonella* and *Yersinia* occupy and replicate within membrane-bound vacuoles, while other invasive bacteria, including *Shigella*, *Listeria*, and *Burkholderia*, are able to escape from endocytic vacuoles to reside within the host cell cytoplasm (1). The precise intracellular localization of internalized bacteria relies on the expression of specific virulence factors, as well as the ability of the bacteria to acquire essential nutrients from the host (1). Because intracellular bacterial metabolism relies on either the uptake of resources for *de novo* synthesis or the direct exploitation of host metabolites, defining the nutritional requirements for intracellular bacterial replication can provide valuable insight into the establishment and progression of infection.

Uropathogenic *Escherichia coli* (UPEC), the predominant cause of urinary tract infections (UTIs) (2, 3), has a transient intracellular lifestyle within terminally differentiated superficial bladder epithelial cells during the acute phase of infection (4, 5). This intracellular stage begins with UPEC attachment to mannosylated receptors on the urothelium, primarily via adhesive fibers called type 1 pili (6, 7). Binding, as well as stochastic internalization during contraction of the bladder during voiding (8), leads to bacterial internalization. The majority of internalized UPEC is nonlytically regurgitated

into the bladder lumen via a Toll-like receptor 4 (TLR4)-dependent mechanism (9, 10). However, if a bacterium escapes expulsion, it clonally expands within the host cell cytosol, forming a biofilm-like multicellular structure comprising 10^4 to 10^5 tightly packed UPEC cells (4, 5). These structures, termed intracellular bacterial communities (IBCs), are held together by type 1 pili (11) and exhibit differential gene expression reminiscent of that of biofilms (12). Similar to biofilms, bacteria within IBCs are protected from host cell insults and can disperse to secondary sites, facilitating disease propagation and adverse disease outcomes such as recurrence and chronic symptomatic colonization (12–14).

Few investigations have probed UPEC nutritional requirements during acute UTI. Previous studies have demonstrated a requirement for amino acid utilization during acute UTI and have indicated that UPEC, despite being a facultative anaerobe, requires aerobic respiration to establish infection (15–18). Transcriptional studies investigating the profiles of UPEC during acute infection also revealed increased expression of siderophores, indicative of iron limitation and/or electron scavenging for aerobic respiration, as well as utilization of alternative carbon sources (15, 19, 20). However, these studies did not capture requirements for nucleotide metabolism pathways.

One limitation to the identification of UPEC factors that are critical for intracellular survival is the UPEC pathogenic cascade itself, which comprises several bottlenecks that preclude the use of large-scale *in vivo* screens. In murine models of acute UTI, 10 million bacteria are instilled via transurethral catheterization to the bladder lumen, and of these, the vast majority are eliminated by micturition (12). Of approximately 1,000 bacteria that adhere to the bladder epithelial cells, only about 100 will become IBC progenitors (12). To partially surpass these limitations, a transposon mutagenesis analysis identified several IBC effectors through the screening of UPEC mutants defective for *in vitro* biofilm formation under multiple growth and nutrient conditions (21). Among the factors identified as modulators of biofilm formation was the inner membrane protein colicin V production accessory protein (CvpA) (21). This finding was intriguing because loss of CvpA impacted biofilm formation without impairing production of type 1 pili, which are considered to be the paramount adhesive fiber during biofilm formation *in vivo* (21). In UPEC, *cvpA* is localized within an operon upstream of the purine biosynthesis-associated gene *purF* (22). PurF catalyzes the first committed step in the *de novo* purine biosynthesis pathway, which is essential for cellular replication under conditions in which bacteria are unable to scavenge for exogenous nucleotides. Disruption of *de novo* purine biosynthesis has been shown to attenuate the virulence of several intracellular pathogens, including *Salmonella*, *Burkholderia*, *Brucella*, and *Francisella* (23–26). Thus far, the role of *de novo* purine synthesis in UPEC pathogenesis has not been elucidated.

Here, we investigated the function of CvpA and PurF in UPEC pathogenesis. We report that *de novo* purine biosynthesis is critical for bacterial proliferation within the bladder epithelial cell cytosol and demonstrate preliminary evidence that CvpA may play a contributing role in the bacterial defense against neutrophil-mediated killing.

RESULTS

Production of PurF depends on the presence of *cvpA*. A previous transposon mutant library screen generated in the cystitis isolate UTI89 identified several determinants required for *in vitro* biofilm formation, including *cvpA* (21). Unmarked, clean deletion of *cvpA* recapitulated *in vitro* biofilm phenotypes of the Tn::*cvpA* mutant, further demonstrating a role of *cvpA* in biofilm development (21). Previous work had mapped the transcriptional start site of the *purF* gene, encoding the corresponding *de novo* purine biosynthesis enzyme PurF, to a region upstream of the operon containing *cvpA* (22, 27). However, real-time quantitative PCR (qPCR) analysis of statically grown UTI89 cultures revealed that in comparison to wild-type (WT) UTI89, the unmarked Δ*cvpA* mutant produced levels of *purF* transcript that were decreased by approximately 15-fold (Fig. 1A), despite genetic maintenance of the previously mapped *cvpA-purF* transcriptional start site (22, 27). Further scrutiny of the literature revealed that *purF*

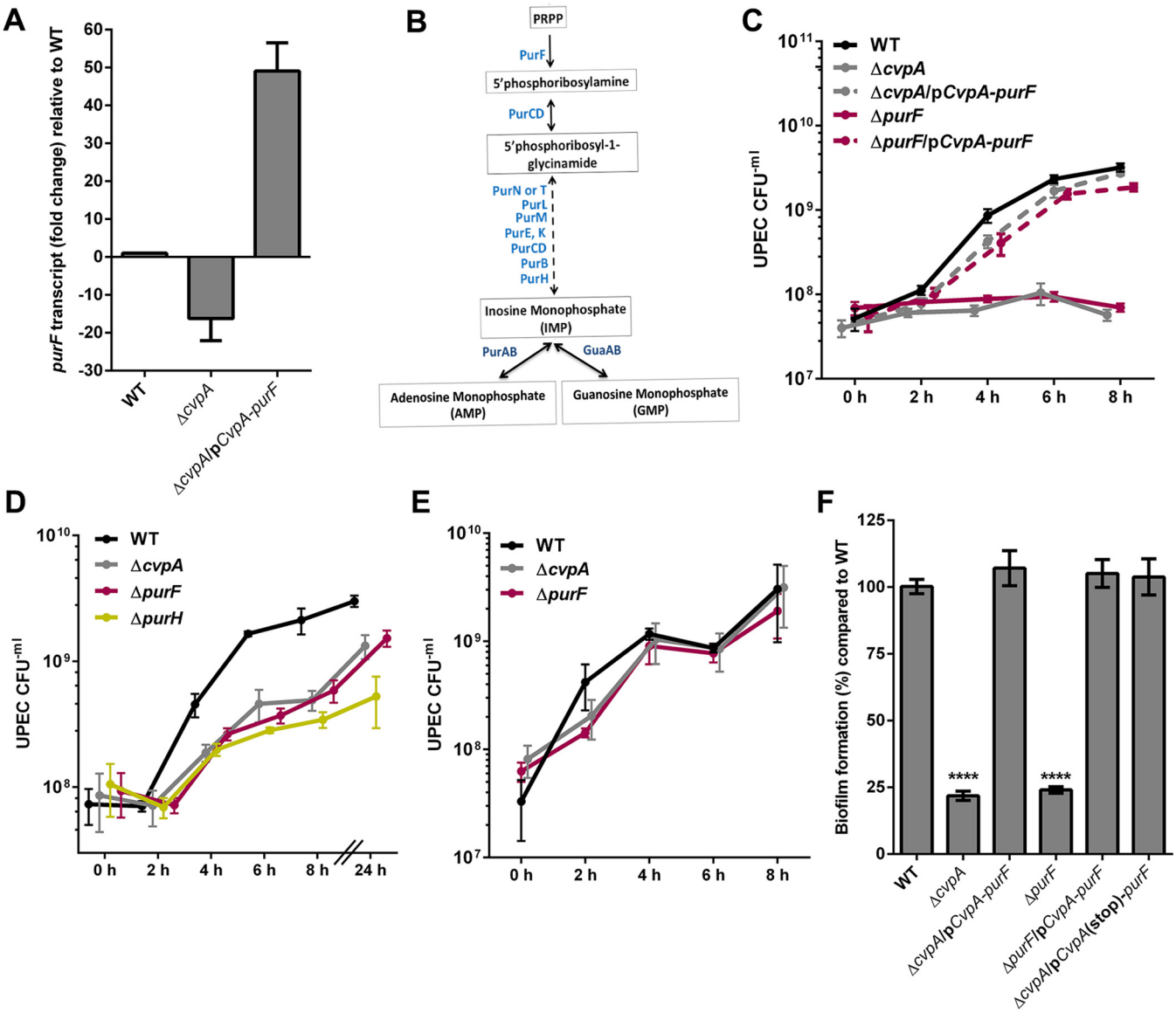

FIG 1 UPEC *cvpA-purF* is required for purine biosynthesis and biofilm formation. (A) qPCR evaluating steady-state transcript levels of *purF* in statically grown UTI89 cultures. The graph depicts relative the fold change of the *purF* transcript normalized to levels of *gyrB* and compared to WT UTI89. (B) Schematic representation of the *de novo* purine biosynthesis pathway in *E. coli* (adapted from KEGG pathway analysis). PRPP, phosphoribosyl pyrophosphate. (C) Growth of UTI89 mutants in M9 minimal medium. (D) Metabolic complementation of UTI89 isogenic mutants deficient in *de novo* purine biosynthesis. (E) Growth of purine biosynthesis mutants in human urine. In panels C to E, graphs depict the average CFU per milliliter of bacterial culture at the indicated time points, and data represent the mean ± standard error of the mean (SEM) for at least three independent experiments. (F) UPEC biofilm formation in YESCA-PVC. The graph depicts the percent biofilm production by each strain compared to the WT UTI89 OD_{565} reading, which represents 100%. Bars represent the mean biofilm production ± SEM for at least three independent experiments. The *P* values in panel F were calculated by one-way ANOVA with Dunnett's *post hoc* correction for multiple comparisons to WT values. ****, $P < 0.0001$.

expression was linked to the production of *cvpA* (22, 27). Given that the sequences encoding *cvpA-purF* are nearly identical in UTI89 and the previously reported strains, we hypothesized that the *cvpA* deletion impaired expression of *purF*. Indeed, steady-state levels of *purF* transcript were approximately 40-fold greater when Δ*cvpA* was complemented with a plasmid harboring the *cvpA-purF* operon under the control of the endogenous promoter (Δ*cvpA/pcvpA-purF*) than for the WT (Fig. 1A).

PurF catalyzes the addition of an amino group derived from glutamine to the C-1 position of phosphoribosyl pyrophosphate (PRPP) in the first committed step of *de novo* purine biosynthesis (28) (Fig. 1B). To evaluate *de novo* purine biosynthesis *in vitro*, we evaluated the ability of the Δ*cvpA* mutant to replicate in M9 minimal medium, which is devoid of exogenous purines. As expected, the Δ*cvpA* mutant was unable to replicate

in the absence of exogenous purines (Fig. 1C). Bacterial replication in M9 medium was restored to WT levels in the Δ*cvpA*/p*cvpA-purF* strain (Fig. 1C). The replication defects of a Δ*purF* clean deletion mutant mirrored those of the Δ*cvpA* mutant, and likewise, Δ*purF* could be rescued by complementation with p*cvpA-purF* (Δ*purF*/p*cvpA-purF*) (Fig. 1C).

IMP is the product of the purine metabolism enzyme *purH* (Fig. 1B), and it represents a branch point of the purine biosynthetic pathway that can be converted into either AMP or GMP (Fig. 1B). Both the Δ*cvpA* and Δ*purF* mutants were able to reach final cell densities close to that of the WT in M9 medium supplemented with IMP, reaching 10^9 CFU/ml of culture (Fig. 1D) and demonstrating that these mutants can sufficiently take up exogenous metabolites required to complete the final steps of *de novo* purine biosynthesis. As a control, a UTI89 Δ*purH* mutant, which was also previously reported to exhibit biofilm formation defects (21), could be metabolically complemented by the addition of IMP to minimal medium (Fig. 1D). Collectively, these data established that *cvpA* mutants are purine auxotrophs due to ablation of *purF* expression in the Δ*cvpA* background. Furthermore, both the Δ*purF* and Δ*cvpA* mutants proliferated in human urine (Fig. 1E), suggesting that the purine content within the urine can sustain growth of UTI89 Δ*cvpA-purF* and isogenic derivatives and implying that the bladder lumen could serve as a replicative niche for these isogenic mutants.

Purine biosynthetic pathways are required for UPEC biofilm formation *in vitro*. Given that a previous study identified *cvpA* and *purH* as UPEC biofilm effectors under *in vitro* conditions (21) we next sought to analyze the effects of the *purF* deletion on *in vitro* biofilm production. Both Tn::*cvpA* and Tn::*purH* mutants were previously shown to have altered production of curli adhesive fibers (21). Consistent with previous studies, UTI89 Δ*cvpA* was unable to form biofilms under conditions with yeast extract-Casamino Acids (YESCA) medium and polyvinyl chloride (PVC) (Fig. 1F), which promote a biofilm that depends primarily on the expression of curli and cellulose (29). Notably, UTI89 Δ*cvpA* exhibits a moderate growth defect during growth in YESCA medium (21). The growth and biofilm defects in this medium could be rescued by *cvpA-purF* genetic complementation (Fig. 1F). Similarly, the Δ*purF* mutant was unable to form biofilms in YESCA medium, and this phenotype was rescued by extrachromosomal expression of *cvpA-purF* (Fig. 1F). In order to evaluate the specific contribution of CvpA in biofilm formation, we introduced a stop codon within the *cvpA* coding region of the p*cvpA-purF* plasmid [p$cvpA_{(STOP)}$-*purF*] and introduced this plasmid into the Δ*purF* strain [Δ*purF*/p$cvpA_{(STOP)}$-*purF*]. Under the tested conditions, the Δ*purF*/p$cvpA_{(STOP)}$-*purF* strain formed biofilms at WT levels, thus demonstrating that CvpA is dispensable during *in vitro* biofilm formation (Fig. 1F) and that *de novo* purine biosynthesis is required for biofilm formation during growth in YESCA medium. Mutants deficient in purine biosynthetic pathways exhibited WT motility levels (see Fig. S1 in the supplemental material), indicating that the observed biofilm defects are not due to an alteration in the production of flagella. In total, these data indicate that disruption of *cvpA* imparts a polar mutation that significantly decreases *de novo* purine biosynthesis and that endogenous purine synthesis, but not CvpA production, is required for UTI89 biofilm formation *in vitro*. Because our studies demonstrate that clean deletion of the *cvpA* gene impairs *purF* transcription, below we denote UTI89 Δ*cvpA* as UTI89 Δ*cvpA-purF*.

Purine biosynthesis mutants elaborate type 1 pili and adhere to immortalized bladder epithelial cells *in vitro*. UPEC adherence is the first step leading to infection within the urinary tract. If a mutation impairs adherence, the IBC cascade is confounded during infection (11). We therefore sought to investigate the impact of impaired purine biosynthesis on UPEC interactions with human bladder epithelial cells (BECs). Previous studies have demonstrated that type 1-piliated UPEC can adhere to and become internalized within cultured BECs, including the 5637 bladder carcinoma cell line (6, 13).

Adherence assays revealed that loss of *purF* alone, or loss of both *cvpA* and *purF*, did not alter the ability of UPEC to adhere to BECs (Fig. 2A). Immunoblot analyses probing for the primary pilin subunit FimA indicated that all strains tested in adherence and internalization studies produced FimA levels that were similar to those produced by WT

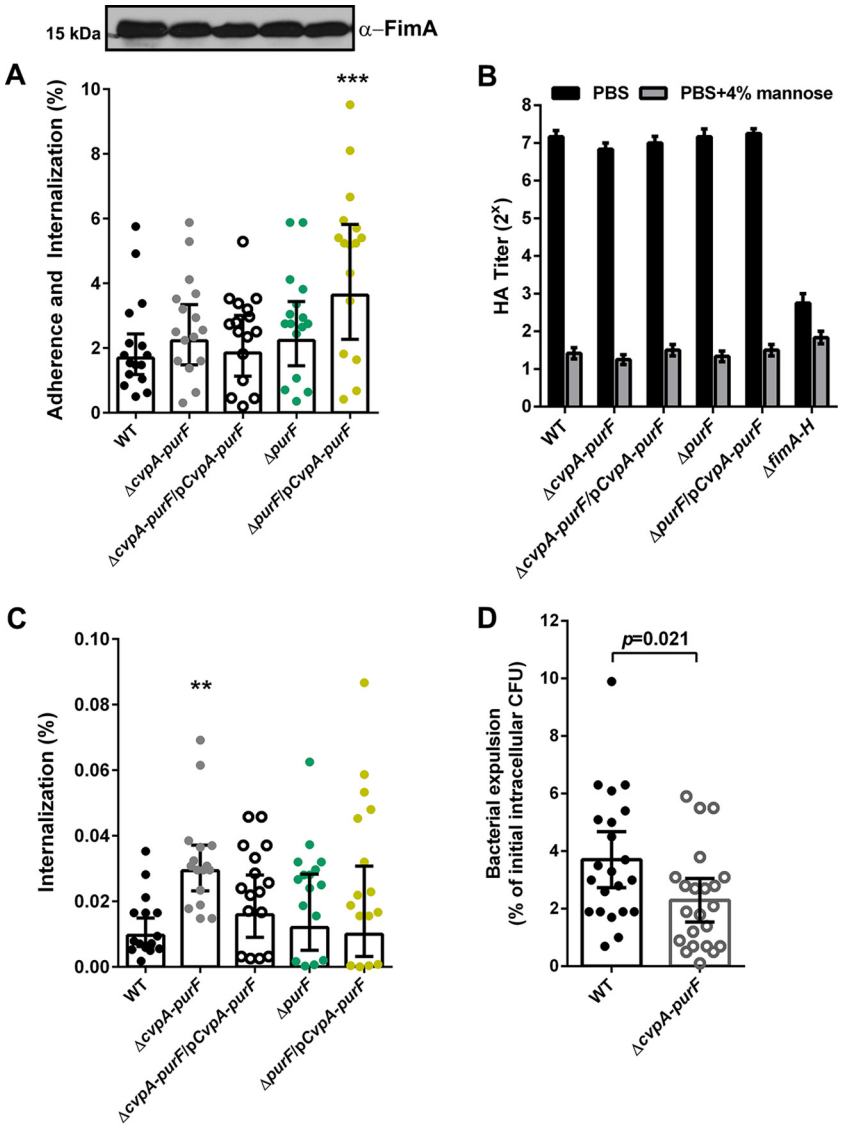

FIG 2 Purine biosynthesis modulates bacterial adherence and entry into bladder epithelial cells. 5637 bladder epithelial cells (BECs) were cultured with the indicated UPEC strain. (A) Quantification of total adherent (cell-associated) and intracellular UPEC bacteria. The graph depicts the geometric mean (bars) and 95% confidence interval (whiskers) of bacterial titers recovered from BEC monolayers expressed as a percentage of total UPEC bacteria recovered from control wells for at least five independent experiments. Inset, immunoblot depicting production of the type 1 pilus major subunit FimA by each UTI89 strain (α-FimA). (B) Hemagglutination (HA) of guinea pig erythrocytes, measuring assembly of type 1 pili adhesive fibers by the indicated UTI89 strain in the presence or absence of mannose. PBS, phosphate-buffered saline. The graph depicts the average HA titer of guinea pig red blood cells by mannose-sensitive type 1 pili obtained in two independent experiments. (C) Percentage of UTI89 strains internalized by BECs by 2 h postinfection. The graph depicts the geometric mean (bars) and 95% confidence interval (whiskers) of internalized bacterial titers expressed as a percentage of total CFU recovered from control wells from at least five biological replicate experiments. (D) BEC expulsion of internalized UPEC was assayed at 4 h after gentamicin treatment. Data are expressed as the geometric mean (bars) and 95% confidence interval (whiskers) of the percentage of total internalized UPEC expelled into cell culture supernatants following gentamicin treatment. In panels A and C, *P* values were calculated by one-way ANOVA with Dunnett's *post hoc* correction for multiple comparisons to WT values. ***, $P < 0.001$; **, $P < 0.01$. The *P* values in panel D were calculated by two-tailed *t* test.

UTI89 (Fig. 2A, inset). Interestingly, the adherence levels of the Δ*purF*/p*cvpA-purF* strain exceeded those of WT UTI89, suggesting that excess *cvpA-purF* expression augments bacterial adherence. To understand the basis of enhanced bacterial adherence observed in the Δ*purF*/p*cvpA-purF* strain, we assayed the extent of piliation in the Δ*purF*/p*cvpA-purF* strain, using an indirect approach. UPEC elaborating type 1 pili can

agglutinate guinea pig red blood cells in a type 1 pilus-dependent manner via interactions of the tip adhesin FimH with mannosylated receptors on the erythrocyte surface (30); thus, the addition of mannose in hemagglutination (HA) reactions can sequester FimH-producing bacteria to unmask the production of additional fibers that may agglutinate erythrocytes (30). In our hemagglutination assays, all strains exhibited similar mannose-sensitive HA titers (Fig. 2B), suggesting that differential expression of type 1 pili or production of other appendages that can agglutinate guinea pig red blood cells is not a contributing factor to the increased BEC binding exhibited by the Δ*purF/*p*cvpA-purF* strain.

UPEC purine auxotrophs exhibit altered rates of bacterial expulsion from immortalized human BECs. The adherence assays demonstrated that purine biosynthesis mutants have no defect in the production of type 1 pili, which are critical for UPEC adhesion to the bladder epithelial surface. Using gentamicin protection assays, we next analyzed the number of internalized bacteria for each strain. In these assays, the Δ*purF* and Δ*purF/*p*cvpA-purF* mutants were internalized at levels that were not statistically significantly different than those of WT UTI89 (Fig. 2C). Notably, the Δ*cvpA-purF* strain was consistently internalized at significantly higher levels than WT UTI89 (Fig. 2C); genetic complementation of Δ*cvpA-purF* restored bacterial internalization titers to WT levels (Fig. 2C). The basis of the observed increased internalization into human bladder epithelial cells remains unknown.

When UPEC enters BECs, a TLR4-mediated defense mechanism that leads to nonlytic expulsion of UPEC is triggered (9). UPEC cells that are expelled from BECs can further be encased within host membrane-derived vesicles that contain caveolin-1 and Rab27b (9, 10). We therefore investigated whether loss of *cvpA-purF* alters the dynamics of bacterial expulsion by BECs. BEC monolayers were infected with either the WT or Δ*cvpA-purF* strain for 1 h, followed by gentamicin treatment to eliminate extracellular bacteria. At this point, gentamicin-protected monolayers in replicate wells were lysed, and initial intracellular titers were determined for each strain (corresponding to time zero). To the remaining wells, bacteriostatic sulfamethoxazole and D-mannose were added to prevent bacterial replication and *fim*-mediated reattachment and entry, respectively. Following 4 h of incubation, we determined the number of extracellular UPEC bacteria by enumeration of CFU expelled into the cell culture supernatants. This time point was previously shown to correspond with peak UPEC expulsion from BECs (10). At 4 h after gentamicin treatment, we found that compared to the WT, fewer Δ*cvpA-purF* bacteria were present in the cell culture supernatant (Fig. 2D). These data suggest that there is reduced expulsion of Δ*cvpA-purF* bacteria into the cell culture medium, which is potentially due to less efficient recognition by the innate immune response.

Purine biosynthesis promotes UPEC colonization of the bladder. We next sought to analyze the contribution of *de novo* purine synthesis in bacterial colonization and intracellular expansion in a murine model of acute UTI. Female 7- to 8-week-old C3H/HeN mice were transurethrally inoculated with the WT, Δ*cvpA-purF*, or Δ*cvpA-purF/*p*cvpA-purF* strain as previously described (31), and bladder bacterial burdens were recorded at 3, 6, and 16 h postinfection, marking the acute stages of the UPEC pathogenic cascade (5). In comparison to WT UTI89, the Δ*cvpA-purF* (Fig. 3A) and Δ*purF* (Fig. 3C) mutants were significantly impaired in their ability to colonize the bladder, and this defect was rescued by extrachromosomal genetic complementation.

In the murine model of UTI employed in our studies, UPEC adheres to BECs and becomes internalized within 3 h postinfection, with vacuolar escape and expansion into IBCs occurring by 6 h postinfection. While the *in vitro* studies preceding the mouse infections suggested that expression of type 1 pili (which is critical for UPEC adherence [7] and IBC cohesion [11]) was unaltered in the Δ*cvpA-purF* strain, it is possible that this mutant displays a piliation defect *in vivo*. To evaluate this possibility, we generated a Δ*cvpA-purF* deletion in UTI89 *fim*LON, a previously constructed strain in which the phase-variable *fim* promoter element (32) is genetically locked into the transcriptionally

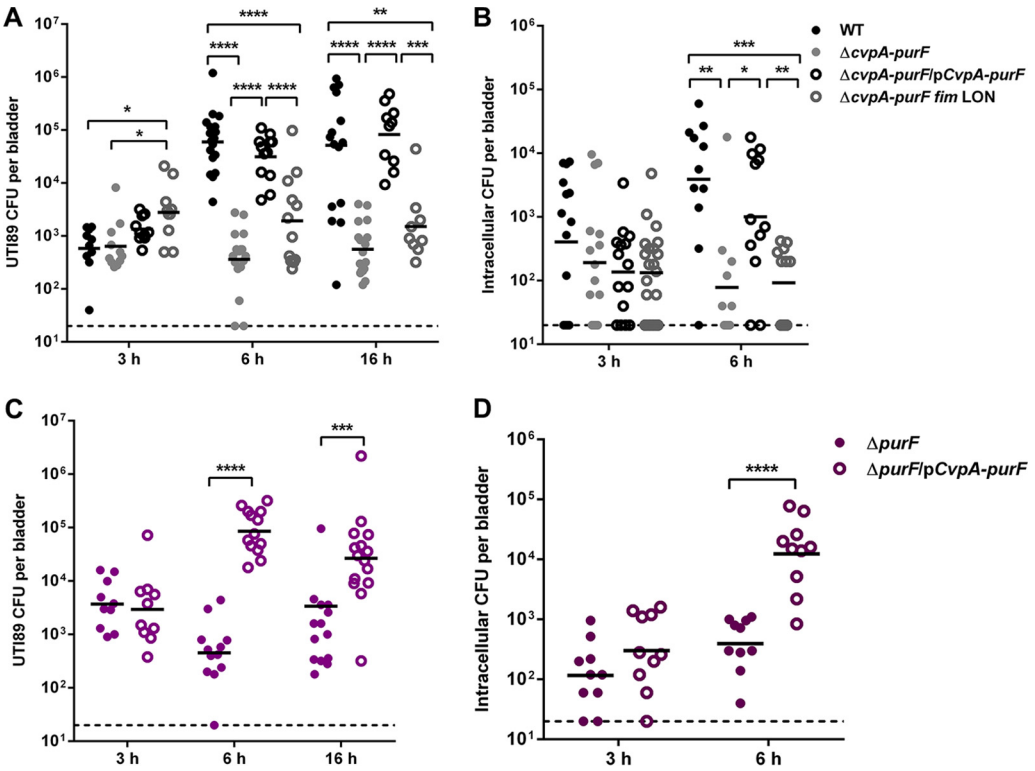

FIG 3 UTI89 purine auxotrophs are attenuated in a murine model of acute urinary tract infection. (A) Bladder bacterial titers recovered from C3H/HeN mice infected with the indicated UTI89 strain at 3, 6, and 16 h postinfection. (B) Intracellular bacterial titers recovered from whole gentamicin-treated bladders infected with UTI89 *cvpA-purF* mutants at the indicated time points of infection. (C) Bladder bacterial titers obtained from C3H/HeN mice infected with the indicated *purF* mutant. (D) Intracellular bacterial titers recovered from whole gentamicin-treated bladders infected with the indicated *purF* mutant at 3 and 6 h postinfection. The lines in all panels represent the geometric mean of the distribution, and each circle represents bacterial CFU recovered from one individual mouse bladder. *P* values were calculated by the two-tailed Mann-Whitney *t* test. ****, $P < 0.0001$; ***, $P < 0.001$; **, $P < 0.01$; *, $P < 0.05$.

competent state (33). Subsequent analyses of the fitness of the resulting strain *in vivo* revealed that compared to those of WT UTI89, the UTI89 Δ*cvpA-purF fim*LON bladder titers remained significantly reduced (Fig. 3A), suggesting that reduced bladder colonization by purine biosynthesis mutants is not due to defects in differential transcription of the *fim* operon *in vitro* and *in vivo*.

We next determined the intracellular population of each UPEC strain during the early stages of UTI. Using gentamicin treatment to eliminate extracellular bacteria from the excised bladder, we observed that at 3 h postinfection, the intracellular numbers of all UPEC strains lacking *cvpA-purF* were slightly lower (but not statistically significantly different) than the intracellular numbers obtained for WT UTI89 (Fig. 3B). By 6 h postinfection, the intracellular titers of the Δ*cvpA-purF* (Fig. 3B), Δ*cvpA-purF fim*LON (Fig. 3B), and Δ*purF* (Fig. 3D) strains were dramatically reduced compared to those of either WT or the corresponding complemented strains, indicating that *de novo* purine biosynthesis plays a critical role in UPEC expansion in the intracellular compartment.

Purine biosynthesis mutants exhibit a minor defect in vacuolar escape. One critical step of the UPEC pathogenic cascade that remains poorly characterized is the mechanism by which bacteria exit the endocytic vacuole. Previous studies have employed chloroquine resistance assays to discriminate vacuolar versus cytosolic Gram-negative bacteria (34, 35). Aiming to better understand the defect observed in the murine studies described above, we adapted the chloroquine resistance assay and evaluated its potential use as a tool to discriminate between internalized vacuolar and cytoplasmic UPEC subpopulations. In initial, proof-of-principle studies, we combined gentamicin and chloroquine resistance assays to determine the proportion of UPEC bacteria that enter the cytoplasm of cultured human BECs. Treatment of UPEC-infected

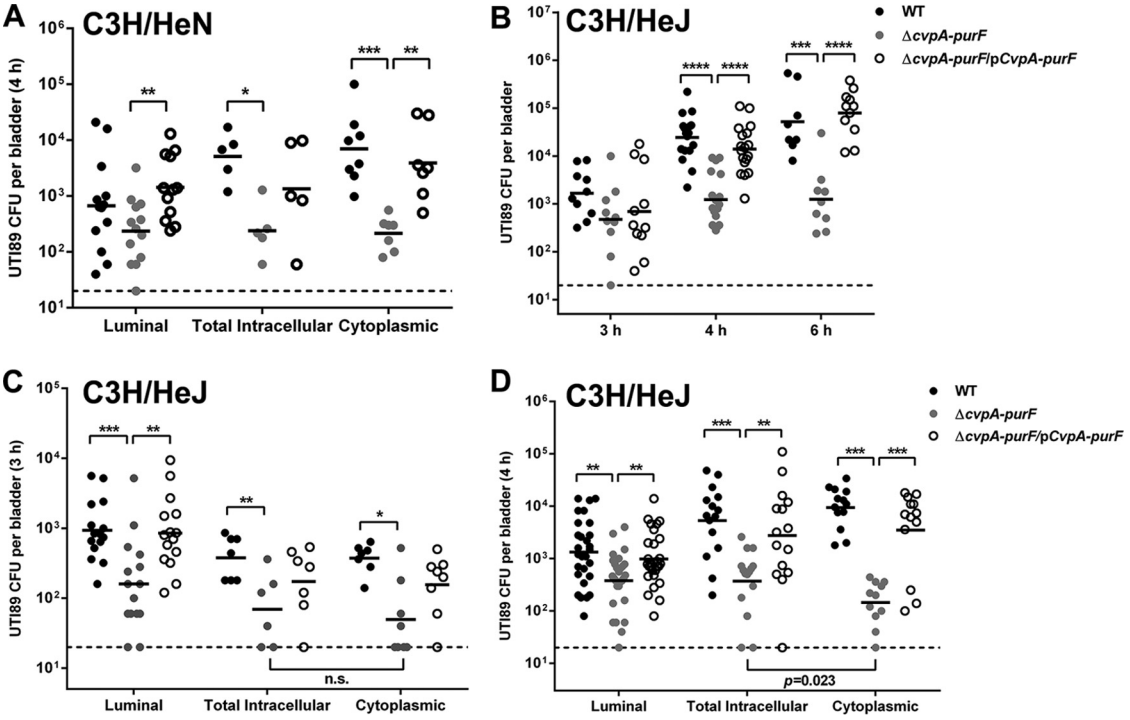

FIG 4 *De novo* purine biosynthesis is required for bacterial expansion in the urothelial cell cytoplasm. (A) Chloroquine and gentamicin protection assays were utilized to enumerate bacterial titers recovered from C3H/HeN bladder compartments at 4 h postinfection. (B) Total bacterial titers recovered from C3H/HeJ whole bladders infected for 3, 4, or 6 h with the indicated UTI89 strain. (C) Gentamicin and chloroquine resistance assays were utilized to enumerate the bacterial CFU contained within each C3H/HeJ bladder cell partition at 3 h postinfection (early acute infection). (D) Bacterial titers recovered from gentamicin- and chloroquine-treated C3H/HeJ bladders at 4 h postinfection (bacterial cytoplasmic expansion and early IBC formation). Lines represent the geometric mean of each distribution, and each circle represents bacterial titers recovered from one individual mouse. *P* values were calculated by the Mann-Whitney *t* test. ****, $P < 0.0001$; ***, $P < 0.001$; **, $P < 0.01$; *, $P < 0.05$.

BECs with gentamicin in combination with chloroquine revealed distinct subpopulations of bacteria within BECs that presumably localize to the BEC cytoplasm (see Fig. S2A in the supplemental material). At high concentrations (2.5 mg/ml [34]), chloroquine treatment only slightly reduced the viability of planktonic UPEC in batch culture (Fig. S2B), while chloroquine treatment of intracellular UPEC in cultured BECs reduced the recoverable bacterial titers by 20- to 100-fold (Fig. S2A). Consistent with previous reports, these studies indicate that chloroquine reaches an active threshold concentration within host cell vacuoles that is sufficient to perturb the viability of vacuole-bound intracellular UPEC. Thus, a gentamicin and chloroquine resistance assay allows for the compartmental discrimination of UPEC due to concentration of lysosomotropic chloroquine in UPEC-containing vacuoles to levels that reduce the viability of intravacuolar bacteria (35), while the concentration of chloroquine within the host cell cytoplasm remains insufficient to significantly perturb bacterial viability (34, 36). In cultured BECs, we observed significantly decreased resistance of the Δ*cvpA-purF* strain to chloroquine treatment compared to that of either the WT or Δ*cvpA-purF/pcvpA-purF* strain (Fig. S2A). These data suggest that fewer Δ*cvpA-purF* bacteria are localized to the host cell cytosol in the cultured BECs at the tested time point, suggesting that in this *in vitro* assay, purine biosynthesis mutants may exhibit delayed or impaired egress from host cell vacuoles.

We next investigated the intravacuolar and cytoplasmic subpopulations of internalized UPEC in the murine bladder. For these studies, we used gentamicin treatment to determine the overall intracellular bacterial titers at 3 h (Fig. 3B) and 4 h (Fig. 4A) postinfection. At both time points, the Δ*cvpA-purF* mutant exhibited reduced intracellular titers, although the reduction of recoverable titers at 3 h was not statistically different from that for the WT (Fig. 3B). By 4 h postinfection, a time point at which

escape from the vacuole has occurred and IBC expansion is under way (5), we observed a statistically significant reduction in total intracellular Δ*cvpA-purF* titers compared to those of either WT or Δ*cvpA-purF/pcvpA-purF* strain (Fig. 4A). However, chloroquine resistance assays utilized to determine the number of bacteria localized to the host cell cytosol revealed that the Δ*cvpA-purF* titers did not significantly differ from those recovered for total intracellular Δ*cvpA-purF* bacteria (Fig. 4A). These data suggest that in contrast to the case in cultured human BECs, the majority of intracellular purine biosynthesis mutants are localized to the host cell cytoplasm by 4 h postinfection and do not exhibit an apparent defect in exiting the endocytic vacuole.

We next analyzed the ability of purine biosynthesis mutants to colonize C3H/HeJ mice, which fail to respond to lipopolysaccharide (LPS) due to a point mutation within the *tlr4* locus (37). These experiments were aimed at examining whether TLR4 activation contributes to reduced cytosolic proliferation of the Δ*cvpA-purF* mutant. Transurethral inoculations followed by CFU analyses indicated that compared to the WT, Δ*cvpA-purF* bladder titers were decreased in C3H/HeJ mice by 4 h postinfection (Fig. 4B), and remained consistently low at 6 h postinfection, similar to bacterial colonization observed in C3H/HeN mice. Similarly, at 3 h postinfection, luminal and total intracellular Δ*cvpA-purF* titers were markedly reduced compared to those of either the WT or Δ*cvpA-purF/pcvpA-purF* strain (Fig. 4C). Bacterial subcellular localization studies using gentamicin and chloroquine resistance assays indicated a modest (3.5-fold) reduction in the recovery of cytosolic Δ*cvpA-purF* CFU in chloroquine-treated bladders compared to total intracellular bacteria at 4 h postinfection in this mouse background (Fig. 4D). Conversely, the number of WT and Δ*cvpA-purF/pcvpA-purF* bacteria localized to the host cell cytoplasm did not differ from total intracellular titers (Fig. 4D). These observations suggested that in C3H/HeJ mice, UTI89 Δ*cvpA-purF* may exhibit a defect or a delay in vacuolar escape. Taken together, these data suggest that *de novo* purine biosynthesis is required for bacterial replication and expansion within the bladder epithelial cell cytosol.

DISCUSSION

The capacity of the vertebrate host to deprive intracellular bacteria of essential nutrients and metabolites is a powerful innate immune defense mechanism. Within the host, a transient intracellular lifestyle enables UPEC to remain shielded from antibiotic intervention and subvert host surveillance mechanisms that are recruited to the site of infection. Here, we show that UPEC requires *de novo* purine biosynthesis to expand within the cytoplasm of superficial bladder facet cells during acute UTI. In order to establish acute UTI and progress to later stages of infection, UPEC must overcome several critical bottlenecks, including avoidance of the host immune response, entry into the superficial bladder epithelium, and escape from the endocytic vacuole in which the bacterium is encased. The mechanism and factors driving UPEC escape from the vacuole are unknown. While other intracellular pathogens deploy needle-like appendages associated with type III or type IV secretion systems to manipulate the host cell and facilitate intravacuolar survival and/or escape (1), these systems are rarely harbored by uropathogenic *E. coli*. Although several toxins have been described as UPEC virulence factors, including hemolysin A (38), none of these factors are essential for UPEC manipulation of the host vacuolar space or for UPEC escape into the host cell cytosol. One previous study exploring the metabolic requirements of UPEC growth during UTI identified guanine biosynthesis as essential for growth in human urine and virulence during experimental murine infection (39), and another study discovered that loss of pyrimidine nucleotide synthesis led to attenuation of UPEC survival within the urinary tract (40). In contrast, our data demonstrate that UTI89 mutants lacking intact purine biosynthetic pathways can replicate in human urine (Fig. 1E).

Disruption of bacterial purine biosynthesis pathways has been shown to play a role in the niche colonization and intracellular lifestyle of other pathogens, including *Burkholderia pseudomallei* (26), *Brucella abortus* (25), *Salmonella enterica* serovar Typhimurium (24, 41), *Campylobacter jejuni* (42), *Francisella tularensis* (23, 43), and *Listeria*

monocytogenes (44). Although these pathogens harbor *cvpA* and *purF* orthologs, genetic colocalization of the *cvpA-purF* loci is not universally maintained. Interestingly, the *cvpA-purF* operon is conserved among UPEC strains, as well as strains of other uropathogens, including *Klebsiella pneumoniae* and *Proteus mirabilis*. We speculate that maintenance of *cvpA-purF* genetic synteny in UPEC isolates may reflect a specialized role of *cvpA* during colonization of the urinary tract. In addition, these studies surmise that the host cell cytosol contains limiting amounts of essential purine metabolites that are available for import into intracellular bacteria; thus, *de novo* purine biosynthesis is crucial for bacterial replication within this nutrient-starved environment. The lack of purine nucleotides within the host cell cytoplasm may therefore serve as a metabolic cue that can be sensed by UPEC to signal that the bacterium has reached the cytosol.

Our studies indicated that in a TLR4-competent mouse strain, vacuolar escape is not impeded by the lack of an intact purine biosynthetic pathway. Future studies will interrogate mechanisms that facilitate UPEC escape from the vacuole. Recent transcriptome sequencing (RNA-seq) analyses investigating the UPEC transcriptome during the middle stage of IBC formation (6 h postinfection) identified highly activated alternative carbon source pathways but did not pinpoint upregulation of *de novo* purine synthesis (19). Consistent with these studies, sampling of bacterial mRNA isolated from the acute stages of infection did not identify upregulation of *cvpA-purF* during infection, suggesting a posttranscriptional mode of regulation (data not shown).

Previous work has suggested that defective purine metabolism can render bacteria more susceptible to the oxidative burst, presumably because of an inability to repair damage cause by reactive oxygen species (24). CvpA was previously shown to be essential for the production of colicin V (22), a small peptide antibiotic (a "bacteriocin") that kills *E. coli* cells by inserting into the inner membrane and disrupting membrane potential (45). *E. coli* produces many different types of bacteriocins with diverse killing mechanisms, and the genes encoding each bacteriocin are typically coexpressed with cognate transport systems (46). In UPEC strains, studies demonstrated that bacteriocins and other pore-forming toxins such as α-hemolysin (HlyA) are upregulated during infection and contribute to pathogenesis (38, 47). For example, HlyA is capable of suppressing the host inflammatory response through disruption of NF-κB signaling, degradation of the cytoskeletal scaffolding protein paxillin, and attenuation of macrophage chemotaxis (38, 47). However, the involvement of CvpA in these toxin-mediated processes remains unexplored. While CvpA is conserved among *E. coli* strains, the repertoire of bacteriocins and hemolysins harbored by each strain varies depending on plasmid content and the type and number of pathogenicity islands present in the chromosome of each isolate. It is thus possible that CvpA is critical for the secretion of several different bacteriocins or toxins or that it has an additional function that warrants genetic conservation across strains. In future studies, we will aim to characterize the contribution of CvpA to the secretion of UPEC toxin repertoires. Preliminary studies probing the effects of CvpA on UPEC survival against polymorphonuclear leukocytes (PMNs) suggest a modest defect of a strain lacking CvpA (see Fig. S3 in the supplemental material). In summary, this work demonstrates that the *cvpA-purF* locus is required for optimal UPEC intracellular replication and expansion into IBCs during acute UTI in murine infection models. We demonstrate that *de novo* purine synthesis is required after UPEC internalization into bladder epithelial cells, suggesting that the urothelial cell cytosol restricts purine availability and, in turn, constrains bacterial survival within the intracellular niche.

MATERIALS AND METHODS

Bacterial strains and constructs. UTI89 (and derivatives thereof) is a UPEC cystitis isolate (13) used in all of the studies described here. UTI89 *fim*LON is a previously constructed isogenic strain in which the left invertible repeat that serves as a recognition site for *fim* promoter recombination and inversion has been mutated (preventing the ON→OFF inversion) (33). UTI89 nonpolar isogenic gene deletions were constructed using the λ Red recombinase system following the method of Murphy and Campellone (48). UTI89 Δ*cvpA* and UTI89 Δ*purH* were previously generated and characterized (21). A UTI89 Δ*purF* isogenic mutant was generated using the λ Red recombinase system and primers *purF*-KO_Left (5′-TCATCCTTCGTTATGCATTTCGAGATTTTCCACTTCGTTCTGACGTTGCAGTGTAGGCTGGAGCTGC

TTC-3′) and *purF*-KO_Right (5′-CGATGATCATCGGCCACGGTATGGTTGCTTTCCGCGATCCTAACGGGATT CTATGAATATCCTCCTTAG-3′). Deletion of *purF* was confirmed using test primers Test_KO*purF* R (5′-CACTACCCGCTGGAAGCC-3′) and Test_KO*purF*_L (5′-GCCCTGTCAGACTTGCAGG-3′). UTI89 Δ*cvpA* and UTI89 Δ*purF* were complemented by transformation via electroporation with pTRC99A containing the *cvpA-purF* locus under the control of the native promoter upstream of *cvpA* (22, 27). The resulting complementation construct, p*cvpA-purF*, was generated by amplifying *cvpA-purF* from UTI89 using primers *cvpA_purF*_pTRC99AF (5′-CGGAATTCTCATCCTTCGTTATGCATTTCGAG-3′) and *cvpA_purF*_pTRC99AR (5′-CGA AGCTTCCAGCGCGTCTTATCAGGCCTGTGCTGG-3′) and cloning of the amplicon into pTRC99A by BamHI/HindIII restriction digestion (NEB) and ligation by T4 DNA ligase (Promega). Site-directed mutagenesis using primers *cvpA*_stop_F (5′-GGCCAGTTGGTGGAGTAAACGGGGTTGTCAGGCACC-3′) and *cvpA*_stop_R (5′-GGTGCCTGACAACCCCGTTTACTCCACCAACTGGCC-3′) was used to insert the stop codon TAA within the *cvpA* coding region [p$cvpA_{(STOP)}$-*purF*] using p*cvpA-purF* as a template. UTI89 strains harboring either empty pTC99A (vector-only controls) or *cvpA-purF* constructs were maintained in lysogeny broth (LB) supplemented with 100 μg/ml ampicillin.

Growth curves. All overnight cultures described in this work were seeded in LB and incubated at 37°C with shaking. For growth curves, overnight cultures were used to seed either M9 minimal medium (1× M9 salts, 2 mM $MgSO_4$, 0.1 mM $CaCl_2$, 0.4% glucose, 50 μg/ml niacin) or M9 medium supplemented with 40 mM IMP (Sigma) at an optical density at 600 nm (OD_{600}) of 0.1. Cultures were incubated with shaking at 37°C, and aliquots were taken at 60-min intervals for OD_{600} measurements and CFU enumeration by serial dilution plating. Analysis of UPEC growth in human urine was performed on pooled, filtered, sterilized urine, which was collected under the Vanderbilt Institutional Review Board (IRB) protocol (151465) and filtered through a 0.22-μm-pore-size filter before use.

***In vitro* biofilm assays.** UTI89 strains grown overnight in LB as described above were diluted 1:1,000 in fresh LB and grown to an OD_{600} of 1. Strains were subcultured (1:500) in yeast extract-Casamino Acids (YESCA) medium and used to seed 96-well PVC plates. Biofilm formation was quantified after a 48-h static incubation at room temperature (ranging from 23 to 24°C), using the colorimetric crystal violet method as previously described (21). Biofilm formation by each strain was normalized to the WT UTI89 OD_{570} reading, which was scaled to 100% for each independent biological replicate plate. Statistical analysis was performed using at least three independent biological replicates for each strain, using one-way analysis of variance (ANOVA) with multiple comparisons to WT values and Dunnett's *post hoc* correction.

Immunoblot analysis. UTI89 strains, statically incubated at 37°C in LB medium for 48 h (with subculturing after 24 h into fresh LB), were used for evaluation of type 1 pilus production. Cultures were normalized to an OD_{600} of 1, and 1 ml of each normalized culture was pelleted and concentrated 10× in 1× SDS buffer containing 1 M HCl. Cell lysates were boiled for 5 min to dissociate assembled type 1 pili and immediately neutralized with 1 M NaOH. Equivalent volumes of each sample were analyzed by SDS-PAGE. Membranes were blotted using antiserum raised against type 1 pili (FimA) (49) at a 1:5,000 dilution.

RNA extraction, DNase treatment, reverse transcription, and qPCR. Bacterial cultures were grown as described for immunoblot analysis. Extraction of bacterial RNA was performed using the Qiagen RNeasy kit and quantified on a NanoDrop 2000c instrument. One-microgram samples were DNase I treated using Turbo DNase I (Ambion) and verified as devoid of DNA using PCR and a series of primers annealing to the *rrsH* gene. Reverse transcription of 0.5 μg of DNase-treated sample from each strain was performed using SuperScript II reverse transcriptase (Life Technologies) according to the manufacturer's protocol and as described previously (33). The reverse-transcribed product was purified and quantified using a NanoDrop 2000c instrument and used for quantitative PCR (qPCR) analysis with TaqMan chemistry (50). Determination of relative fold changes between different strains and the wild-type control was performed following the $\Delta\Delta C_T$ method of Pfaffl (51). For these analyses, we utilized 25 ng cDNA template. Triplicate wells per sample were used for the analysis. Standard controls were incorporated in each analysis, including DNase I-treated RNA samples (no reverse transcriptase), and DNA (positive) controls for each primer set and probe. The primers and probe sets used were as follows: gene of interest (GOI), *purF* (probe, 5′-6FAM-CCGCTATGTTGGCCG-3′; primers, *purF*_F [5′-CCGCCATCGCTGCTACA-3′] and *purF*-R [5′-TCATCGCCACACAGGCATA-3′]); housekeeping normalizer gene *gyrB* (probe, 5′VIC-ACGAACT GCTGGCGGA-3′). Reactions were multiplexed for every experiment. qPCR analyses were performed a total of three times, sampling 3 independent biological replicate cultures.

Bacterial adherence and internalization assays. 5637 (ATCC HTB-9) bladder epithelial cells were seeded in 24-well plates and grown to confluence in complete RPMI 1640 medium (Gibco) supplemented with 10% fetal bovine serum (Atlanta Biologicals). Bacterial strains were grown as described for immunoblot analysis and normalized to an OD_{600} of 0.5 in sterile phosphate-buffered saline (PBS). In triplicate wells, bladder epithelial cells were infected at a multiplicity of infection (MOI) of approximately 20 bacteria per epithelial cell. To synchronize bacterial adherence, tissue culture plates were centrifuged at 600 × *g* for 5 min, and plates were incubated at 37°C in 5% CO_2 for 2 h. To determine the number of adherent and intracellular UPEC bacteria, one set of triplicate wells was washed 5 times with PBS to remove nonadherent bacteria, and monolayers were lysed by the addition of 0.1% Triton X-100 and mechanical disruption to release intracellular bacteria. Tenfold serial dilutions of cell culture lysates were plated on LB agar for enumeration of CFU. In parallel, triplicate wells were processed for total bacterial titers at 2 h postinfection by the addition of Triton X-100 (final concentration, 0.1%), mechanical disruption, and plating of 10-fold serial dilutions on LB agar. To determine the number of intracellular UPEC bacteria, a set of triplicate wells was washed 3 times in sterile PBS, followed by the addition of fresh RPMI containing 100 μg/ml gentamicin (Gibco) to kill extracellular bacteria. After another 2 h of incubation at 37°C in 5% CO_2, wells were washed 3 times in sterile PBS to remove cellular debris and

gentamicin, and monolayers were lysed by the addition of 0.1% Triton X-100 and mechanical disruption. Tenfold serial dilutions of cell culture lysates were plated on solid LB agar, and intracellular bacterial titers were determined by enumeration of CFU. Triplicate wells were processed for total bacterial titers at 4 h postinfection by the addition of Triton X-100 (final concentration, 0.1%) with mechanical disruption and plating of 10-fold serial dilutions on LB agar. Bacterial adherence and internalization are expressed as a percentage of the total bacterial titers for each independent experiment, with each assay performed a minimum of three times.

HA assays. Bacteria were grown as described for immunoblot analysis studies. Production of type 1 pili was assessed by hemagglutination (HA) of guinea pig erythrocytes as previously described (30), using bacterial cultures that were normalized to an OD_{600} of 1. Guinea pig red blood cells were obtained from the Colorado Serum Company. In parallel, HA assays were conducted using PBS containing 4% mannose to discriminate among type 1 pili (mannose-sensitive HA) and other adhesive fibers. Data are representative of two independent biological replicate experiments with each sample assayed in duplicate.

Bacterial expulsion assay. Bacteria were grown and prepared for infection as described for BEC adherence assays. Bacterial expulsion was determined as described previously (10). Briefly, 5637 cell monolayers were infected at an MOI of 100 in triplicate, and after 1 h, monolayers were washed with sterile PBS to remove nonadherent bacteria. Monolayers were incubated in fresh RPMI containing 100 μg/ml gentamicin for 1 h at 37°C, followed by several washes with sterile PBS. At this time point (corresponding to 0 h), six wells infected by each strain were lysed by addition of 0.1% Triton X-100 to determine the initial level of intracellular bacteria. To the remaining wells, RMPI medium containing 100 mM D-mannose and 25 μg/ml of the bacteriostatic reagent trimethoprim (Sigma) was added to prevent bacterial reattachment and replication. Cocultures were incubated for an additional 4 h. At the end of the incubation, 50 μl of culture supernatant was collected from each well and plated on solid LB to determine expelled bacterial titers. The percentage of extracellular bacteria at 4 h was calculated relative to the intracellular bacterial load at 0 h, and values were expressed as percent bacterial fluxing. Each assay was repeated 3 times, and each independent experiment contained six replicate wells per strain.

Mouse infection studies. Seven- to 9-week-old female C3H/HeN or C3H/HeJ mice (Harlan) were transurethrally inoculated with 10^7 CFU of each UTI89 strain as previously described (33). To ensure the proper and humane treatment of animals, all animal studies were carried out in strict accordance with the recommendations in the *Guide for the Care and Use of Laboratory Animals* of the National Institutes of Health (52) and the Vanderbilt University Medical Center's Institutional Animal Care and Use Committee (IACUC), who approved all protocols. Bacterial colonization was assessed by plating 10-fold serial dilutions of whole-bladder homogenates and enumerating the recoverable CFU. Bacterial titers represent the total luminal, adherent, and intracellular bacteria in each whole bladder. Statistical analyses were performed using the two-tailed Mann-Whitney *t* test.

Whole-bladder gentamicin protection assay. At the indicated infection time points, bladders were aseptically removed, bisected, and washed twice in sterile PBS. Washes were pooled and plated for enumeration of CFU to determine luminal bacterial titers. Washed bladders were incubated in 100 μg/ml gentamicin for 90 min at 37°C with gentle shaking to kill adherent extracellular bacteria. Bladders were washed in sterile PBS to remove debris and residual gentamicin and were subsequently homogenized in sterile PBS. Serial dilutions of bladder homogenates were plated on solid LB agar to enumerate intracellular bacterial titers.

Chloroquine resistance assays. The 5637 bladder epithelial cell line (ATCC HTB-9) was used for chloroquine resistance assays. Cells were seeded in 24-well tissue culture dishes and grown to confluence as described for the adherence and internalization assays. UPEC cells were normalized to an OD_{600} of 0.5 in sterile PBS and were inoculated into six replicate wells at an MOI of 20. Tissue culture plates were centrifuged at 600 $\times$ *g* to synchronize bacterial adherence, and the plates were incubated at 37°C in 5% CO_2 for 2 h. Cell monolayers were washed twice with sterile PBS to remove nonadherent bacteria. For each strain, one set of six replicate wells was incubated in RPMI containing 100 μg/ml gentamicin, and in parallel, a set of six replicate wells was treated with RPMI containing 100 μg/ml gentamicin and 2.5 mg/ml chloroquine (Sigma) for 90 min at 37°C. After antibiotic treatment, cell monolayers were washed three times in sterile PBS, and BEC monolayers were lysed by addition of 0.1% Triton X-100. Bacterial titers were enumerated by plating 10-fold serial dilutions on LB agar. For determination of the chloroquine resistance of planktonically grown bacteria, UPEC strains were grown in LB with shaking at 37°C to mid-log phase (~4 h). Bacterial cultures were normalized to an OD_{600} of 0.3 in sterile PBS or PBS containing 2.5 mg/ml chloroquine and were subsequently incubated at 37°C with gentle shaking for 90 min. Bacterial survival was determined by enumerating CFU (10-fold serial dilutions) on LB agar. Data are representative of at least 2 independent biological replicate experiments.

For whole-bladder analyses, mice were infected with the indicated UPEC strain for 3 to 4 h prior to euthanasia and aseptic removal of the bladder. Bladders were bisected and washed to determine luminal bacterial titers as described for whole-bladder gentamicin protection assays. Washed bladders were then incubated in sterile PBS containing 100 μg/ml gentamicin and 2.5 mg/ml chloroquine for 90 min at 37°C with gentle shaking. Gentamicin- and chloroquine-treated bladders were washed in PBS to remove residual antibiotic and were homogenized in sterile PBS. Intracellular bacterial titers were enumerated by plating serially diluted bladder homogenates on LB agar. For all chloroquine resistance assays, graphs depict the geometric mean of recovered bacterial titers, and statistical analyses were performed using the two-tailed Mann-Whitney *t* test.

SUPPLEMENTAL MATERIAL

Supplemental material for this article may be found at https://doi.org/10.1128/IAI.00471-16.

TEXT S1, PDF file, 0.5 MB.

ACKNOWLEDGMENTS

We thank Timothy Cover for the use of specialized equipment.

The authors declare no competing interests. The content is solely the responsibility of the authors and does not necessarily represent the official views of the NIH.

C.L.S. and M.H. conceptualized and designed the experiments. C.L.S., E.W.Z., A.G.D., D.P.C., B.R.E.A.D., and K.A.F. performed experiments. E.J.B. and K.R.G. provided technical support. D.B.C. and H.M.S.A. contributed essential reagents and isolated PMNs. C.L.S., D.B.C., H.M.S.A., and M.H. analyzed data. C.L.S. and M.H. wrote the manuscript.

REFERENCES

1. Ray K, Marteyn B, Sansonetti PJ, Tang CM. 2009. Life on the inside: the intracellular lifestyle of cytosolic bacteria. Nat Rev Microbiol 7:333–340. https://doi.org/10.1038/nrmicro2112.
2. Griebling TL. 2007. Urologic diseases in America, vol 07-5512. NIH, Washington, DC.
3. Foxman B. 2010. The epidemiology of urinary tract infection. Nat Rev Urol 7:653–660. https://doi.org/10.1038/nrurol.2010.190.
4. Anderson GG, Palermo JJ, Schilling JD, Roth R, Heuser J, Hultgren SJ. 2003. Intracellular bacterial biofilm-like pods in urinary tract infections. Science 301:105–107. https://doi.org/10.1126/science.1084550.
5. Justice SS, Hung C, Theriot JA, Fletcher DA, Anderson GG, Footer MJ, Hultgren SJ. 2004. Differentiation and developmental pathways of uropathogenic *Escherichia coli* in urinary tract pathogenesis. Proc Natl Acad Sci U S A 101:1333–1338. https://doi.org/10.1073/pnas.0308125100.
6. Martinez JJ, Mulvey MA, Schilling JD, Pinkner JS, Hultgren SJ. 2000. Type 1 pilus-mediated bacterial invasion of bladder epithelial cells. EMBO J 19:2803–2812. https://doi.org/10.1093/emboj/19.12.2803.
7. Mulvey MA, Lopez-Boado YS, Wilson CL, Roth R, Parks WC, Heuser J, Hultgren SJ. 1998. Induction and evasion of host defenses by type 1-piliated uropathogenic *Escherichia coli*. Science 282:1494–1497. https://doi.org/10.1126/science.282.5393.1494.
8. Apodaca G. 2004. The uroepithelium: not just a passive barrier. Traffic 5:117–128. https://doi.org/10.1046/j.1600-0854.2003.00156.x.
9. Song J, Bishop BL, Li G, Grady R, Stapleton A, Abraham SN. 2009. TLR4-mediated expulsion of bacteria from infected bladder epithelial cells. Proc Natl Acad Sci U S A 106:14966–14971. https://doi.org/10.1073/pnas.0900527106.
10. Miao Y, Li G, Zhang X, Xu H, Abraham SN. 2015. A TRP channel senses lysosome neutralization by pathogens to trigger their expulsion. Cell 161:1306–1319. https://doi.org/10.1016/j.cell.2015.05.009.
11. Wright KJ, Seed PC, Hultgren SJ. 2007. Development of intracellular bacterial communities of uropathogenic *Escherichia coli* depends on type 1 pili. Cell Microbiol 9:2230–2241. https://doi.org/10.1111/j.1462-5822.2007.00952.x.
12. Schwartz DJ, Chen SL, Hultgren SJ, Seed PC. 2011. Population dynamics and niche distribution of uropathogenic *E. coli* during acute and chronic urinary tract infection. Infect Immun 79:4250–4259. https://doi.org/10.1128/IAI.05339-11.
13. Mulvey MA, Schilling JD, Hultgren SJ. 2001. Establishment of a persistent *Escherichia coli* reservoir during the acute phase of a bladder infection. Infect Immun 69:4572–4579. https://doi.org/10.1128/IAI.69.7.4572-4579.2001.
14. Hannan TJ, Mysorekar IU, Hung CS, Isaacson-Schmid ML, Hultgren SJ. 2010. Early severe inflammatory responses to uropathogenic *E. coli* predispose to chronic and recurrent urinary tract infection. PLoS Pathog 6:e1001042. https://doi.org/10.1371/journal.ppat.1001042.
15. Alteri CJ, Smith SN, Mobley HL. 2009. Fitness of *Escherichia coli* during urinary tract infection requires gluconeogenesis and the TCA cycle. PLoS Pathog 5:e1000448. https://doi.org/10.1371/journal.ppat.1000448.
16. Hadjifrangiskou M, Kostakioti M, Chen SL, Henderson JP, Greene SE, Hultgren SJ. 2011. A central metabolic circuit controlled by QseC in pathogenic *Escherichia coli*. Mol Microbiol 80:1516–1529. https://doi.org/10.1111/j.1365-2958.2011.07660.x.
17. Floyd KA, Moore JL, Eberly AR, Good JA, Shaffer CL, Zaver H, Almqvist F, Skaar EP, Caprioli RM, Hadjifrangiskou M. 2015. Adhesive fiber stratification in uropathogenic *Escherichia coli* biofilms unveils oxygen-mediated control of type 1 pili. PLoS Pathog 11:e1004697. https://doi.org/10.1371/journal.ppat.1004697.
18. Floyd KA, Mitchell CA, Eberly AR, Colling SJ, Zhang EW, DePas W, Chapman MR, Conover M, Rogers BR, Hultgren SJ, Hadjifrangiskou M. 9 May 2016. The UbiI (VisC) aerobic ubiquinone synthase is required for expression of type 1 pili, biofilm formation, and pathogenesis in uropathogenic *Escherichia coli*. J Bacteriol https://doi.org/10.1128/JB.00030-16.
19. Conover MS, Hadjifrangiskou M, Palermo JJ, Hibbing ME, Dodson KW, Hultgren SJ. 2016. Metabolic requirements of *Escherichia coli* in intracellular bacterial communities during urinary tract infection pathogenesis. mBio 7:e00104-16. https://doi.org/10.1128/mBio.00104-16.
20. Reigstad CS, Hultgren SJ, Gordon JI. 2007. Functional genomic studies of uropathogenic *Escherichia coli* and host urothelial cells when intracellular bacterial communities are assembled. J Biol Chem 282:21259–21267. https://doi.org/10.1074/jbc.M611502200.
21. Hadjifrangiskou M, Gu AP, Pinkner JS, Kostakioti M, Zhang EW, Greene SE, Hultgren SJ. 2012. Transposon mutagenesis identifies uropathogenic *Escherichia coli* biofilm factors. J Bacteriol 194:6195–6205. https://doi.org/10.1128/JB.01012-12.
22. Fath MJ, Mahanty HK, Kolter R. 1989. Characterization of a *purF* operon mutation which affects colicin V production. J Bacteriol 171:3158–3161.
23. Chong A, Wehrly TD, Child R, Hansen B, Hwang S, Virgin HW, Celli J. 2012. Cytosolic clearance of replication-deficient mutants reveals *Francisella tularensis* interactions with the autophagic pathway. Autophagy 8:1342–1356. https://doi.org/10.4161/auto.20808.
24. Mantena RK, Wijburg OL, Vindurampulle C, Bennett-Wood VR, Walduck A, Drummond GR, Davies JK, Robins-Browne RM, Strugnell RA. 2008. Reactive oxygen species are the major antibacterials against *Salmonella* Typhimurium purine auxotrophs in the phagosome of RAW 264.7 cells. Cell Microbiol 10:1058–1073. https://doi.org/10.1111/j.1462-5822.2007.01105.x.
25. Alcantara RB, Read RD, Valderas MW, Brown TD, Roop RM, 2nd. 2004. Intact purine biosynthesis pathways are required for wild-type virulence of *Brucella abortus* 2308 in the BALB/c mouse model. Infect Immun 72:4911–4917. https://doi.org/10.1128/IAI.72.8.4911-4917.2004.
26. Pilatz S, Breitbach K, Hein N, Fehlhaber B, Schulze J, Brenneke B, Eberl L, Steinmetz I. 2006. Identification of *Burkholderia pseudomallei* genes required for the intracellular life cycle and *in vivo* virulence. Infect Immun 74:3576–3586. https://doi.org/10.1128/IAI.01262-05.
27. Makaroff CA, Zalkin H. 1985. Regulation of *Escherichia coli purF*. Analysis of the control region of a *pur* regulon gene. J Biol Chem 260:10378–10387.
28. Messenger LJ, Zalkin H. 1979. Glutamine phosphoribosylpyrophosphate amidotransferase from *Escherichia coli*. Purification and properties. J Biol Chem 254:3382–3392.
29. McCrate OA, Zhou X, Reichhardt C, Cegelski L. 2013. Sum of the parts: composition and architecture of the bacterial extracellular matrix. J Mol Biol 425:4286–4294. https://doi.org/10.1016/j.jmb.2013.06.022.
30. Hultgren SJ, Schwan WR, Schaeffer AJ, Duncan JL. 1986. Regulation of

production of type 1 pili among urinary tract isolates of *Escherichia coli*. Infect Immun 54:613–620.
31. Hung CS, Dodson KW, Hultgren SJ. 2009. A murine model of urinary tract infection. Nat Protoc 4:1230–1243. https://doi.org/10.1038/nprot.2009.116.
32. Klemm P. 1986. Two regulatory fim genes, *fimB* and *fimE*, control the phase variation of type 1 fimbriae in *Escherichia coli*. EMBO J 5:1389–1393.
33. Kostakioti M, Hadjifrangiskou M, Cusumano CK, Hannan TJ, Janetka JW, Hultgren SJ. 2012. Distinguishing the contribution of type 1 pili from that of other QseB-misregulated factors when QseC is absent during urinary tract infection. Infect Immun 80:2826–2834. https://doi.org/10.1128/IAI.00283-12.
34. Paetzold S, Lourido S, Raupach B, Zychlinsky A. 2007. *Shigella flexneri* phagosomal escape is independent of invasion. Infect Immun 75:4826–4830. https://doi.org/10.1128/IAI.00454-07.
35. Fernandez-Prada CM, Hoover DL, Tall BD, Hartman AB, Kopelowitz J, Venkatesan MM. 2000. *Shigella flexneri* IpaH(7.8) facilitates escape of virulent bacteria from the endocytic vacuoles of mouse and human macrophages. Infect Immun 68:3608–3619. https://doi.org/10.1128/IAI.68.6.3608-3619.2000.
36. Finlay BB, Falkow S. 1988. Comparison of the invasion strategies used by *Salmonella cholerae-suis*, *Shigella flexneri* and *Yersinia enterocolitica* to enter cultured animal cells: endosome acidification is not required for bacterial invasion or intracellular replication. Biochimie 70:1089–1099. https://doi.org/10.1016/0300-9084(88)90271-4.
37. McAdam KP, Ryan JL. 1978. C57BL/10/CR mice: nonresponders to activation by the lipid a moiety of bacterial lipopolysaccharide. J Immunol 120:249–253.
38. Dhakal BK, Mulvey MA. 2012. The UPEC pore-forming toxin alpha-hemolysin triggers proteolysis of host proteins to disrupt cell adhesion, inflammatory, and survival pathways. Cell Host Microbe 11:58–69. https://doi.org/10.1016/j.chom.2011.12.003.
39. Russo TA, Jodush ST, Brown JJ, Johnson JR. 1996. Identification of two previously unrecognized genes (*guaA* and *argC*) important for uropathogenesis. Mol Microbiol 22:217–229. https://doi.org/10.1046/j.1365-2958.1996.00096.x.
40. Bahrani-Mougeot FK, Buckles EL, Lockatell CV, Hebel JR, Johnson DE, Tang CM, Donnenberg MS. 2002. Type 1 fimbriae and extracellular polysaccharides are preeminent uropathogenic *Escherichia coli* virulence determinants in the murine urinary tract. Mol Microbiol 45:1079–1093. https://doi.org/10.1046/j.1365-2958.2002.03078.x.
41. Leung KY, Finlay BB. 1991. Intracellular replication is essential for the virulence of *Salmonella typhimurium*. Proc Natl Acad Sci U S A 88:11470–11474. https://doi.org/10.1073/pnas.88.24.11470.
42. Cameron A, Huynh S, Scott NE, Frirdich E, Apel D, Foster LJ, Parker CT, Gaynor EC. 2015. High-frequency variation of purine biosynthesis genes is a mechanism of success in *Campylobacter jejuni*. mBio 6:e00612-15. https://doi.org/10.1128/mBio.00612-15.
43. Weiss DS, Brotcke A, Henry T, Margolis JJ, Chan K, Monack DM. 2007. *In vivo* negative selection screen identifies genes required for *Francisella* virulence. Proc Natl Acad Sci U S A 104:6037–6042. https://doi.org/10.1073/pnas.0609675104.
44. Schauer K, Geginat G, Liang C, Goebel W, Dandekar T, Fuchs TM. 2010. Deciphering the intracellular metabolism of *Listeria monocytogenes* by mutant screening and modelling. BMC Genomics 11:573. https://doi.org/10.1186/1471-2164-11-573.
45. Gerard F, Pradel N, Wu LF. 2005. Bactericidal activity of colicin V is mediated by an inner membrane protein, SdaC, of *Escherichia coli*. J Bacteriol 187:1945–1950. https://doi.org/10.1128/JB.187.6.1945-1950.2005.
46. Duquesne S, Destoumieux-Garzon D, Peduzzi J, Rebuffat S. 2007. Microcins, gene-encoded antibacterial peptides from enterobacteria. Nat Prod Rep 24:708–734. https://doi.org/10.1039/b516237h.
47. Gur C, Coppenhagen-Glazer S, Rosenberg S, Yamin R, Enk J, Glasner A, Bar-On Y, Fleissig O, Naor R, Abed J, Mevorach D, Granot Z, Bachrach G, Mandelboim O. 2013. Natural killer cell-mediated host defense against uropathogenic *E. coli* is counteracted by bacterial hemolysinA-dependent killing of NK cells. Cell Host Microbe 14:664–674. https://doi.org/10.1016/j.chom.2013.11.004.
48. Murphy KC, Campellone KG. 2003. Lambda Red-mediated recombinogenic engineering of enterohemorrhagic and enteropathogenic *E. coli*. BMC Mol Biol 4:11. https://doi.org/10.1186/1471-2199-4-11.
49. Kostakioti M, Hadjifrangiskou M, Pinkner JS, Hultgren SJ. 2009. QseC-mediated dephosphorylation of QseB is required for expression of genes associated with virulence in uropathogenic *Escherichia coli*. Mol Microbiol 73:1020–1031. https://doi.org/10.1111/j.1365-2958.2009.06826.x.
50. Guckes KR, Kostakioti M, Breland EJ, Gu AP, Shaffer CL, Martinez CR, III, Hultgren SJ, Hadjifrangiskou M. 2013. Strong cross-system interactions drive the activation of the QseB response regulator in the absence of its cognate sensor. Proc Natl Acad Sci U S A 110:16592–16597. https://doi.org/10.1073/pnas.1315320110.
51. Pfaffl MW. 2001. A new mathematical model for relative quantification in real-time RT-PCR. Nucleic Acids Res 29:e45. https://doi.org/10.1093/nar/29.9.e45.
52. National Research Council. 2011. Guide for the care and use of laboratory animals, 8th ed. National Academies Press, Washington, DC.